THE JOURNAL OF PHYSICAL CHEMISTRY A

ARTICLE

pubs.acs.org/JPCA

New Way of Describing Static and Dynamic Deformations of the Jahn−Teller Type in Ring Molecules

Wenli Zou, Dmitry Izotov, and Dieter Cremer*

Department of Chemistry, Southern Methodist University, 3215 Daniel Avenue, Dallas, Texas 75275-0314, United States

Supporting Information

ABSTRACT: A new method is presented to describe deformations of an *N*-membered planar ring (*N*-ring) molecule in terms of deformation vectors that can be expressed by a set of $2N - 3$ deformation amplitudes and phase angles. The deformation coordinates are directly derived from the normal vibrational modes of the *N*-ring and referenced to a regular polygon (*N*-gon) of unit length. They extend the conceptual approach of the Cremer-Pople puckering coordinates (J. Am. Chem. Soc. 1975, 97, 1354) to the planar ring and make it possible to calculate, e.g., a planar ring of special deformation on a Jahn−Teller surface. It is demonstrated that the $2N - 3$ deformation parameters are perfectly suited to describe the pseudorotation of a bond through the ring as it is found in cyclic Jahn−Teller systems. In general, an *N*-membered planar ring can undergo $N - 2$ different bond pseudorotations provided the energetics of such a process is feasible. The Jahn−Teller distortions observed in ring compounds correspond either directly to the basic pseudorotation modes or to linear combinations of them. Any deformed ring molecule can be characterized in terms of the new ring deformation coordinates, which help to identify specific electronic effects. The usefulness of the ring deformation coordinates is demonstrated by calculating the Jahn−Teller surfaces for bond pseudorotation in the case of the cyclopropyl radical cation and cyclobutadiene as well as the ring deformation surfaces of disulfur dinitride and its dianion employing multireference averaged quadratic coupled cluster (MR-AQCC) theory, equation-of-motion coupled cluster theory in form of EOMIP-CCSD, and single determinant coupled cluster theory in form of CCSD(T).

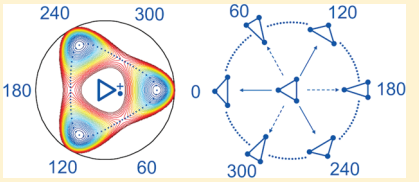

1. INTRODUCTION

A chemical reaction proceeding along a reaction path can be described in its very first stage via a molecular vibration or a combination of molecular vibrations.[1−3] A molecular vibration in turn can be formulated in such a way that it is driven by a leading parameter (an internal coordinate, a symmetry coordinate, a puckering coordinate, etc.).[4−6] Hence, by studying the molecular vibrations of a molecule it is possible to define a reaction coordinate for any change of a molecule or reaction complex. This should provide a possibility of identifying and investigating molecular changes, especially rearrangements, that previously were not known or not well understood.

In this work, we investigate the in-plane vibrations of a planar ring[7,8] because they initiate in-plane deformations or rearrangements of the ring molecule that conserve planarity and lead to new ring forms or ring-opening and acyclic forms. Such processes can be Jahn−Teller distortions,[8,9] bond pseudorotation,[9,10] or the closely related bond shifting in annulenes.[11−16] Bond pseudorotation has been observed in the case of charged small ring molecules whereas bond shifting is typical of larger annulenes. In both cases, experimental and theoretical descriptions have focused on stationary points of the associated potential energy surfaces (PES) rather than exploring the PES along a deformation or rearrangement path. The basic difficulty of describing such a path stems from the definition of generally applicable reaction coordinates. In this work, we will introduce a new concept for describing intrinsic deformations as well as rearrangements of planar rings. In deriving this concept, we will be guided by the previous work on pseudorotation of puckered rings and the description of this process with the help of ring puckering coordinates.[17−22]

The new concept is based on a partitioning of the $(3N - 6)$-dimensional configuration space of an *N*-membered ring molecule ("*N*-ring") into subspaces in which specific ring puckering or ring deformation processes can take place. In view of the fact that ring-puckering can be described in an $(N - 3)$-dimensional subspace,[17,21,22] deformations of a planar *N*-ring should take place in a $(2N - 3)$-dimensional subspace spanned for example by *N* bond lengths and $N - 3$ bond angles. Because there are *N* bond angles in the planar *N*-ring, the choice of $N - 3$ bond angles cannot be unique and therefore it is desirable to specify a special set of $(2N - 3)$ deformation coordinates that complements in the case of a nonplanar *N*-ring the $(N - 3)$ puckering coordinates and helps to describe in-plane deformations of the *N*-ring in a unique way. These ring deformation coordinates (RDCs) can be obtained by analyzing the in-plane vibrational modes and their symmetries for a suitable *N*-membered reference ring, then utilizing the symmetry information to define RDCs applicable to any *N*-ring, and finally associating the electronic structure changes of a ring with

Received: May 5, 2011
Revised: June 7, 2011
Published: July 08, 2011

specific ring deformations or dynamic deformation processes such as bond pseudorotation or bond shifting. In this work, it will be shown that RDCs are useful tools for (i) analyzing the geometry of planar ring molecules, (ii) describing static and dynamic ring distortions caused, for example, by a Jahn−Teller effect, and (iii) calculating deformation surfaces for bond pseudorotation, ring inversion, or bond stretch isomerization.

Results of this work are presented in the following sequence. In section 2, we will define the N-membered reference ring, its configurational space, its molecular vibrations, and its symmetry. Utilizing this analysis, we will derive in section 3 RDCs and present their mathematical foundation. In section 4, ring deformations will be characterized with the help of the RDCs and the concept of bond pseudorotation in Jahn−Teller systems will be discussed. Application of the RDCs will be presented in the following section 5.

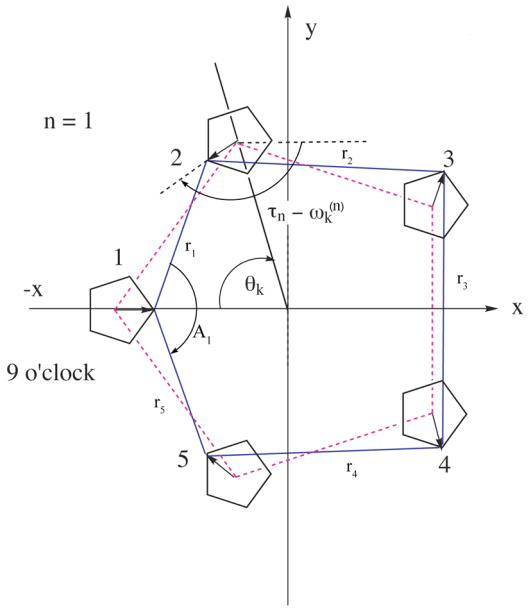

Figure 1. Definition of ring deformation vectors $\mathbf{d}_k$ (included as arrows in the small 5-gons centered at the vertices) for a 5-gon. Symbols used in the text are indicated.

2. SYMMETRY ANALYSIS OF RING VIBRATIONS

Conformational and deformational changes of an N-ring molecule are described by utilizing, as a suitable reference, the N-membered regular polygon ("N-gon") of D_{Nh} symmetry, which we locate in a reference plane called the mean plane (following the nomenclature used for the derivation of ring puckering coordinates[17,21,22]). The normal of the mean plane is chosen to be the z-axis and the mean plane to be identical with the x,y-plane. Furthermore, the geometrical center of the N-gon is used as the origin of the coordinate system. Atom 1 (vertex 1) of the polygon is located at the 9 o'clock position, which gives the direction of the x-axis and the atoms of the polygon are sequentially numbered clockwise around the ring (see the example of a 5-gon in Figure 1).

In general, an N-gon undergoes $3N$ motions, which can be classified with the help of the D_{Nh} character tables for N being even or odd (Tables 1 and 2).[23,24] Because of the positioning of the N-gon in the mean plane and the fixing of the positions of the origin and atom 1, translations and rotations described by the irreducible representations Γ(translation) = A_{2u} + E_{1u} and Γ(rotation) = A_{2g} + E_{1g} for N being even and Γ(translation) = A_2'' + E_1' and Γ(rotation) = A_2' + E_1'' for N being odd, respectively, are frozen (Table 1 and Table 2). There remain $3N - 6$ vibrational motions for the N-gon that split into $N - 3$ (out-of-plane) puckering motions and $2N - 3$ (in-plane) deformation motions. The puckering vibrations are characterized by the irreducible representations $\Gamma(N,\text{even}) = \sum_{m=2}^{N/2-1} E_{m(u,g)} + B_{2(u,g)}$ (for $E_{m(u,g)}$ m even, u; m odd, g; for $B_{2(u,g)}$ $N/2$ even, u; $N/2$ odd, g) and $\Gamma(N,\text{odd}) = \sum_{m=2}^{(N-1)/2} E_m''$ (see also Table A1, Supporting Information). The B_2(u,g) representation produces the out-of-plane displacementes leading to crown conformations (puckered 4-ring with u inversion symmetry, chair of 6-ring with g inversion symmetry, crown forms of 8-, 10-ring, etc.). All other vibrational modes occur in pairs of E-symmetry. It has been shown[17,21,22] that the $N - 3$ out-of plane vibrations with

Table 1. Identification of Ring Motions Using the Character Table for the D_{Nh} Point Group for N Being Even[a]

D_{Nh} (N even)	E	$2(C_N)^n$	C_2	$N/2C_2'$	$N/2C_2''$	0	$2(S_N)^n$	σ_h	$(N/2)\sigma_{d,v}$	$(N/2)\sigma_{v,d}$	ring motion
A_{1g}	+1	+1	+1	+1	+1	+1	+1	+1	+1	+1	breathing
A_{2g}	+1	+1	+1	−1	−1	+1	+1	+1	−1	−1	R_z
B_{1g}	+1	$(-1)^n$	$(-1)^{(N/2)}$	+1	−1	+1	$(-1)^{(N/2)-n}$	$(-1)^{(N/2)}$	+1	−1	deformation
B_{2g}	+1	$(-1)^n$	$(-1)^{(N/2)}$	−1	+1	+1	$(-1)^{(N/2)-n}$	$(-1)^{(N/2)}$	−1	+1	crown puckering
E_{mg}	+2	$2\cos(2mn\pi/N)$	$2(-1)^m$	0	0	+2	$2\cos[(2m(N/2-n)\pi)/N]$	$2(-1)^m$	0	0	m = 1: R_x, R_y
											m = 2, ..., $(N/2) - 1$: deformation; puckering
A_{1u}	+1	+1	+1	+1	+1	−1	−1	−1	−1	−1	
A_{2u}	+1	+1	+1	− 1	−1	−1	−1	−1	+1	+1	T_z
B_{1u}	+1	$(1)^n$	$(-1)^{(N/2)}$	+1	−1	−1	$-(-1)^{(N/2)-n}$	$(-1)^{(N/2)+1}$	−1	+1	deformation
B_{2u}	+1	$(-1)^n$	$(-1)^{(N/2)}$	−1	+1	−1	$-(-1)^{(N/2)-n}$	$(-1)^{(N/2)+1}$	+1	−1	deformation; crown puckering
E_{mu}	+2	$2\cos(2mn\pi/N)$	$2(-1)^m$	0	0	−2	$-2\cos[(2m(N/2-n)\pi)/N]$	$2(-1)^{m+1}$	0	0	m = 1: T_x, T_y; deformation
											m = 2, ..., $(N/2) - 1$: deformation; puckering

[a] n = 1, ..., $(N/2) - 1$; $\sigma_{d,v}/\sigma_{v,d}$ is σ_d/σ_v for $N/2$ being odd and σ_v/σ_d for $N/2$ being even.

dx.doi.org/10.1021/jp2041907 |J. Phys. Chem. A 2011, 115, 8731–8742

Table 2. Identification of Ring Motions Using the Character Table for the D_{Nh} Point Group for N Being Odd[a]

D_{Nh} (N odd)	E	$2(C_N)^n$	NC_2'	σ_h	$2(S_N)^n$	$N\sigma_v$	ring motion
A_1'	+1	+1	+1	+1	+1	+1	breathing
A_2'	+1	+1	−1	+1	+1	−1	R_z
A_1''	+1	+1	+1	−1	−1	−1	
A_2''	+1	+1	−1	−1	−1	+1	T_z
E_m'	+2	$2\cos(2mn\pi/N)$	0	+2	$2\cos(2mn\pi/N)$	0	m = 1: T_x, T_y; deformation
							m = 2, ..., $(N-1)/2$: deformation
E_m''	+2	$2\cos(2mn\pi/N)$	0	−2	$-2\cos(2mn\pi/N)$	0	m = 1: R_x, R_y
							m = 2, ..., $(N-1)/2$: puckering

[a] n = 1, ..., $(N-1)-1$; $\sigma_{d,v}/\sigma_{v,d}$ is σ_d/σ_v for $N/2$ being odd and σ_v/σ_d for $N/2$ being even.

symmetries of the D_{Nh} point group, if frozen at finite vibrational displacements, define $N-3$ basis conformations specified by $N-3$ puckering parameters, which split up in puckering amplitudes q_n and pseudorotation phase angles ϕ_n with $n = m = 2, ..., (N-1)/2$ for N being odd and $n = m = 2, ..., (N-2)/2$ and a single amplitude $q_{N/2}$ for N being even (see Supporting Information, Table A1). In the case of puckering, $n = 0$ and $n = 1$ refer to overall movements of the ring such as translation along the z-axis ($n = 0$) or rotation at axes perpendicular to the z-axis.[21]

There are $2N-3$ in-plane vibrations, of which the ring breathing mode leads to a symmetry-conserving deformation of the polygon ($\Gamma(N,\text{even}) = A_{1g}$; $\Gamma(N,\text{odd}) = A_1'$, Tables 1 and 2) and the remaining $2N-4$ vibrational modes invoke symmetry-changing deformations of the N-gon. All deformation vibrations have to be invariant under the σ_h-symmetry operation of the D_{Nh} group. For N being odd, these are the vibrations with E_m' symmetry and for N being even, vibrations with B_{1g}, B_{2g} (both for $N/2$ even), B_{1u}, B_{2u} (both for $N/2$ odd), E_{mg} for m being even, and E_{mu} for m being odd. Deformation vibrations frozen at finite displacements in line with E-symmetry define ring deformation pairs, which can be described by n pairs of suitable RDCs with $n = 1, ..., (N-2)$. Each ring deformation pair is connected by a dynamic ring deformation process that corresponds to in-plane pseudorotation (see section 4).

In the case of N being odd, there are $(N-1)/2$ E_m'-symmetrical deformation pairs ($m = n = 1, ..., (N-1)/2$) leaving $(N-3)/2$ deformation pairs with $m > (N-1)/2$, which also have to be of E′-symmetry. Because there are no E_m' irreducible representation with $m > (N-1)/2$ in the D_{Nh} group, we define $m' = N - m$ for $m > (N-1)/2$ and specify the missing deformation vibrations to be E_m''-symmetrical. This implies that $(N-3)/2$ ring deformation vibrations (and the corresponding ring deformation processes) can mix because they possess the same symmetry $E_m' = E_m''$ (see section 4).

In the case of N being even, there are $N/2 - 1$ $E_{m(u,g)}$-symmetrical (u for m odd, g for m even) deformation modes. One additional deformation mode can be formed after recognizing that B_{1g}- and B_{2g}-symmetrical vibrations ($N/2$ even) both lead to a lowering from D_{Nh}- to $D_{N/2h}$-symmetry and accordingly form a deformation pair for $m = n = N/2$ as do the B_{1u} and B_{2u}-symmetrical vibrations for $N/2$ being odd. This leaves $(N-4)/2$ deformation pairs unspecified, which we determine, in a way similar to that in the case of the odd-membered rings, by defining $m' = N - m$ for $m = n > N/2$, i.e., $m = n = N/2 + 1, ..., N - 2$. Again, this leads in $(N-4)/2$ cases to the possibility of a mixing of deformation vibrations with the same symmetry. In the following, we will specify the deformation displacements of the vibrational deformation modes by a suitable set of RDCs reflecting the symmetries of the D_{Nh} group.

3. DERIVATION OF RING DEFORMATION COORDINATES

For the purpose of deriving a set of suitable deformation coordinates, the planar N-gon is used as a reference for the corresponding N-ring and specified by a set of initial coordinates. The standard orientation of the N-gon is obtained by choosing the geometrical center of the ring as origin of the coordinate system:

$$\sum_j \mathbf{R}_j^{(0)} = \mathbf{0} \tag{1}$$

where $\mathbf{R}_j^{(0)}$ denotes the position vector of atom j in the N-gon and $j = 1, ..., N$. The reference plane is spanned by vectors $\mathbf{R}'$ and $\mathbf{R}''$ defined in eqs 2 and 3:

$$\mathbf{R}' = \sum_j \mathbf{R}_j^{(0)} \sin\theta_j \tag{2}$$

$$\mathbf{R}'' = \sum_j \mathbf{R}_j^{(0)} \cos\theta_j \tag{3}$$

where the angle θ_j used to rotate position vector $\mathbf{R}_1^{(0)}$ into vector $\mathbf{R}_j^{(0)}$ is given by

$$\theta_j = \frac{2\pi(j-1)}{N} \tag{4}$$

The reference plane is taken to be the xy-plane in the coordinate system of the ring, which means that the unit vector $\mathbf{u}$ defined via the cross product between $\mathbf{R}'$ and $\mathbf{R}''$

$$\mathbf{u} = \frac{\mathbf{R}' \times \mathbf{R}''}{|\mathbf{R}' \times \mathbf{R}''|} \tag{5}$$

points into the direction of the $+z$-axis. When atom 1 is positioned on the $-x$-axis, the coordinate system of the "ring standard orientation" is defined and the positioning of the N-gon in the xy-plane is fixed, thus eliminating any overall rotations and translations (Figure 1).

In the following, it will be useful to set $j - 1 = k$ and renumber all position vectors according to $k = 0, ..., N - 1$. The in-plane deformation of the N-gon at point k can be given by a deformation vector

$$\mathbf{d}_k = d_k^x \mathbf{x}_k + d_k^y \mathbf{y}_k \tag{6}$$

dx.doi.org/10.1021/jp2041907 |J. Phys. Chem. A 2011, 115, 8731–8742

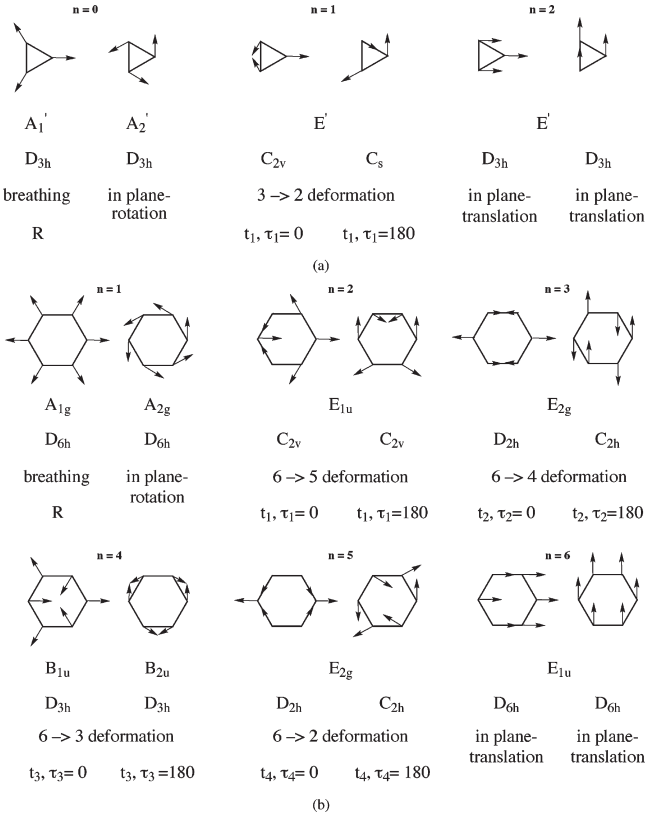

Figure 2. (a) 6 basic in-plane motions of a 3-gon. (b) 12 basic in-plane motions of a 6-gon.

where $\mathbf{x}_k$, $\mathbf{y}_k$ are the local unit vectors at point k, and d_k^x, d_k^y are the associated coordinates. Vectors $\mathbf{R}_k = \mathbf{R}_k^{(0)} + \mathbf{d}_k$ specify the positions of the atoms of an N-gon after deformation (see as an example a 5-gon in Figure 1). The linear space L_k at point k is spanned by vectors $\mathbf{x}_k$ and $\mathbf{y}_k$. The deformation of the N-gon is a vector $\mathbf{d}$ of the linear space L, which is a direct sum of all L_k according to $L = \oplus_{k=0}^{N-1} L_k$, thus implying that $\mathbf{d} = \oplus_{k=0}^{N-1} \mathbf{d}_k$.

The analysis of the deformations of the N-gon depends on the choice of a specific basis in L. We define $\mathbf{x}_k^{(n)}$ and $\mathbf{y}_k^{(n)}$ to be the vectors $\mathbf{x}_k$ and $\mathbf{y}_k$ rotated by the angle $\omega_k^{(n)} = 2\pi(n+1)k/N$, i.e.

$$\mathbf{x}_k^{(n)} = \mathbf{x}_k \cos \omega_k^{(n)} - \mathbf{y}_k \sin \omega_k^{(n)} \tag{7a}$$

$$\mathbf{y}_k^{(n)} = \mathbf{x}_k \sin \omega_k^{(n)} + \mathbf{y}_k \cos \omega_k^{(n)} \tag{7b}$$

A set of all vectors $\mathbf{x}_k^{(n)}$ and $\mathbf{y}_k^{(n)}$ with fixed index n can be regarded as a vector of space L, i.e., $\mathbf{x}^{(n)} = \oplus_k \mathbf{x}_k^{(n)}$ and $\mathbf{y}^{(n)} = \oplus_k \mathbf{y}_k^{(n)}$ are the elements of L. The set of all $\mathbf{x}^{(n)}$ and $\mathbf{y}^{(n)}$, $n = 0, ..., N-1$, form a basis in L. Therefore, an arbitrary planar deformation, $\mathbf{d} = \oplus_k \mathbf{d}_k$, of the N-gon can be written as a linear combination of $\mathbf{x}^{(n)}$ and $\mathbf{y}^{(n)}$,

$$\mathbf{d} = \sum_{n=0}^{N-1} A_n \mathbf{x}^{(n)} + B_n \mathbf{y}^{(n)} \tag{8}$$

$$A_n = N^{-1} \sum_{k=0}^{N-1} d_k^x \cos \omega_k^{(n)} - d_k^y \sin \omega_k^{(n)} \tag{9a}$$

$$B_n = N^{-1} \sum_{k=0}^{N-1} d_k^x \sin \omega_k^{(n)} + d_k^y \cos \omega_k^{(n)} \tag{9b}$$

The coefficients A_n and B_n are the Fourier transforms of coordinates d_k^x and d_k^y. Accordingly, the deformation vector for atom k can be written as

$$\mathbf{d}_k = \sum_n \mathbf{d}_k^{(n)} = \sum_n A_n \mathbf{x}_k^{(n)} + B_n \mathbf{y}_k^{(n)} \tag{10}$$

We shall refer to $\mathbf{d}_k^{(n)}$ as the nth deformation mode at atom k.

One of the advantages of utilizing vectors $\mathbf{x}_k^{(n)}$ and $\mathbf{y}_k^{(n)}$ as basis vectors is that the coefficients A_n and B_n do not depend on the atom index k, and therefore the deformation vectors of the nth mode at each atom of the N-gon have *the same* norm and phase. Figure 2a,b gives schematic representations of the deformation modes of a 3-gon and a 6-gon.

For $n = 0$ in eq 10, the breathing mode and the in-plane rotation mode of the N-gon are obtained. Similarly, the modes with $n = N - 1$ are always translations in the x and y directions, respectively. Hence, the RDCs introduced separate out rotations and translations of the N-gon. The deformation vectors $\mathbf{x}^{(0)}$, $\mathbf{y}^{(0)}$ and $\mathbf{x}^{(N/2)}$, $\mathbf{y}^{(N/2)}$ for even N transform according to 1-dimensional representations A and B, respectively, whereas all other pairs $\mathbf{x}^{(n)}$, $\mathbf{y}^{(n)}$) transform according to 2-dimensional representations E (compare with Tables 1 and 2 or Figure 2a,b). The symmetry group of the N-gon after having encountered the nth mode is found as follows. The breathing, rotational, and translational modes leave the symmetry group unchanged. The deformation modes of the N-gon reduce its symmetry from D_{Nh} to either C_{lh} or D_{lh} ($C_{1h} \equiv C_s$, $D_{1h} \equiv C_{2v}$), where l is the greatest common divisor of n and N. Examples of the symmetry classification are given in Figure 2a,b.

For the purpose of comparing finite deformations in different N-gons, it is convenient to represent the nth deformation mode in the form

$$\mathbf{d}^{(n)} = t_n \cos \tau_n \cdot \mathbf{x}^{(n)} + t_n \sin \tau_n \cdot \mathbf{y}^{(n)} \tag{11}$$

where $t_n = (A_n^2 + B_n^2)^{1/2}$ is the deformation amplitude and $\tau_n = \arctan(B_n/A_n)$ is the phase angle of the nth deformation process. This implies that each deformation vector $\mathbf{d}_k^{(n)}$ has the length t_n and that $\Sigma_k \mathbf{d}_k^{(n)} = 0$ for $n = 1, ..., (N-2)$ of any N-gon. The parameter T determined by

$$T^2 = \sum_n t_n^2 = \sum_n A_n^2 + B_n^2 = \frac{1}{N} \sum_n (d_n^x)^2 + (d_n^y)^2 \tag{12}$$

represents a total planar deformation amplitude ($T \geq 0$). For the case $n = 0$, we specify the radius R of the circumscribed circle of the deformed N-gon via the relationship

$$R^2 = A_0^2 + B_0^2 \tag{13}$$

It is useful to define a breathing deformation amplitude $t_0 = R - R_0$, which compares the radii of the circumscribed cycles of reference N-gon and deformed N-gon. In this way, all $2N - 3$ deformation parameters are specified and their contribution to the actual form of the N-gon can be studied. Computer programs have been written that (i) determine from the Cartesian or internal coordinates of an N-membered ring puckering and deformation coordinates and (ii) build from an input in terms of puckering and deformation coordinates the Cartesian or internal coordinates needed for a quantum chemical calculation.[25,26]

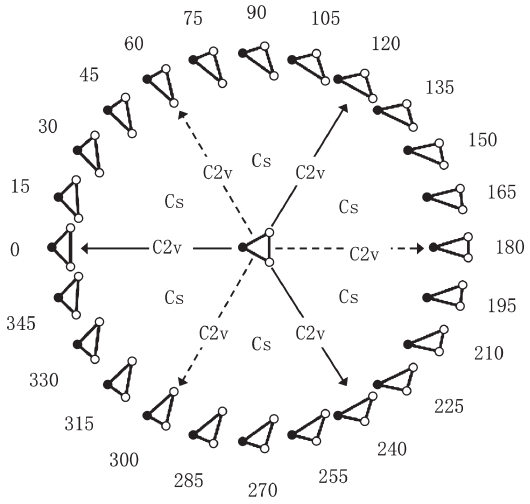

Figure 3. Bond pseudorotation cycle of a 3-gon. The deformed ring forms are shown for a fixed value of t_1 and pseudorotation phase angle τ_1 increasing in steps of 15° from 0 to 360°. The position of atom 1 is indicated by a black dot (clockwise numbering of ring atoms). The basis forms are given by $\tau_1 = 0°$ and 60°. They are formed every 120°.

4. CHARACTERIZATION OF RING DEFORMATION MODES LEADING TO BOND PSEUDOROTATION

One can calculate the Cartesian coordinates of a deformed N-gon for which its RDCs are known via eqs 14 and 15:

$$x_k = -R\cos\omega_k + \sum_{n=1}^{N-2} t_n \cos[\tau_n - \omega_k^{(n)}] \quad (14)$$

$$y_k = R\sin\omega_k + \sum_{n=1}^{N-2} t_n \sin[\tau_n - \omega_k^{(n)}] \quad (15)$$

and all $z_k = 0$. In the case of a puckered N-ring, the out-of-plane deviations are given by eqs 16 and 17[17,21,22]

$$z_k = \sqrt{\frac{2}{N}} \sum_{n=2}^{(N-1)/2} q_n \cos[\phi_n + \omega_k^{(n)}] \qquad (N\ odd) \quad (16)$$

$$z_k = \sqrt{\frac{2}{N}} \sum_{n=2}^{N/2-1} q_n \cos(\phi_n + \omega_k^{(n)}) + \sqrt{\frac{1}{N}} q_{N/2}(-1)^k \qquad (N\ even) \quad (17)$$

where one has to consider that in the case of puckering n starts with 2 and therefore $\omega_k^{(n)} = 2\pi nk/N$. The projection of the puckered ring into the mean plane is given by coordinates $\{\mathbf{x}_k, \mathbf{y}_k\}$ and the associated RDCs of eqs 14 and 15. For the deformed polygons shown in Figures 3 and 4 (see Supporting Information, Figures A1−A4) eqs 14 and 15 have been used directly.

Figures 3 and 4 show the $N - 2$ deformation cycles n of an N-gon with $N = 3$ and 4 where t_n values of 0.3 Å ($R = 1$ Å) and specific τ_n values have been used. Changing the latter in small steps of 15° between 0 and 360°, as done in the case of the 3-ring, provides an impression of how the ring smoothly deforms along the nth deformation process. In other cases, $2N$ specifically deformed N-gons of the nth deformation process have been selected from the infinite number of ring forms generated by increasing τ_n from 0 to 360°. Each deformation process can be characterized by two basis forms in a way that a linear combination of these basis forms generates any other planar ring form in the $\{t_n,\tau_n\}$-subspace. For this purpose, the basis deformation vectors x_n,y_n can be used, which, however, do not lead always to ring forms that can be easily recognizd by the chemist (e.g., $N = 3$, y_1 specifies a C_s-symmetrical form rather than one of the six, easy recognizable C_{2v}-symmetrical forms; see Figure 2a for $n = 1$). Instead, we specify as basis forms the high-symmetry forms with $\tau_n = 0$ and $\tau_n = l\pi/N$, where l is the largest common divisor of N and n as specified in section 2. Each of these basis forms appears N/l times along the deformation cycle in steps of $\Delta\tau_n = 2l\pi/N$. Including the reference N-gon, there are $2N - 3$ basis forms that can be used to generate any deformed N-gon via a linear combination of properly weighted basis forms.

Inspection of the deformed N-gons in Figures 3 and 4 as well as those for the larger N values given in the Supporting Information reveals that the nth deformation mode changes bond lengths and bond angles of the N-gon in such a way that the impression of an $(N - n)$-membered planar ring is provided. In general, an N-gon will approach an $(N - 1)$-gon if one internal angle A_j of the N-gon approaches 180° or, alternatively, one bond length r approaches 0. Hence, a systematic search for widening angles A_j (yielding A_j^+) or decreasing bond lengths r_j (r_j^-) makes it possible to classify a deformation as an $N - 1$, $N - 2$, etc. deformation, i.e., a deformation that gives the impression of reducing the N-gon to an $(N - 1)$-gon, a $(N - 2)$-gon, etc. In this connection it has to be considered that (i) meaningful bond angle/bond length changes have to be distinguished from negligible changes (see Supporting Information) and (ii) A_j^+ and r_j^- changes occurring at the same N-gon vertex or at subsequent N-gon verteces have to be counted only once. In this way, deformation regularities are revealed (see Supporting Information) that specify the nth deformation of an N-gon as effecting n local, disconnected sides of the N-gon and in this way approximating an $(N - n)$-ring, i.e., in the case of $N = 5$, mode $n = 1$ leads to the approximation of a 4-ring, mode 2 to a 3-ring, and mode 3 to a 2-ring. Because a digon contrary to higher polygons does not exist, the deformation leads actually to a stretched or compressed N-gon so that, especially in the case of larger N, the impression of a circle ("digon") deformed (by stretching or compression) to an ellipse results. The analysis of ring deformation is summarized in the Supporting Information.

When the ring deformation mode n for a N-gon changes from $\tau_n = 0$ to $\tau_n = 360°$, the ring form changes in a way than can be viewed in different ways as becomes obvious from inspection of Figure 3: (i) one can follow one particular bond (identified by the numbers of the ring atoms bonded) along a deformation cycle: This bond carrys out a bond stretching vibration (long−short−long). (ii) Alternatively one can follow a bond of about constant length during ring pseudorotation. This bond (e.g., bond 2−3 in the 3-ring given by the light circles) switches at 60, 180, and 300° its position (Figure 3) so that after a full pseudorotation cycle it has moved through the ring to wind up at the starting position. Hence bond pseudorotation is caused by continuous deformation of the ring and bond switching in steps of $l\pi/N$ degrees. Of course, the choice of the reference bond is arbitrary in this connection: Bond 1−2 would have its "rest" positions at 60, 180, and 300° whereas the bond switches would take place at 0, 120, and 240° in the case of the 3-ring. Apart from this it becomes obvious when viewing the deformation cycles of the Supporting Information that for larger N focusing on a specific bond is

dx.doi.org/10.1021/jp2041907 |J. Phys. Chem. A 2011, 115, 8731–8742

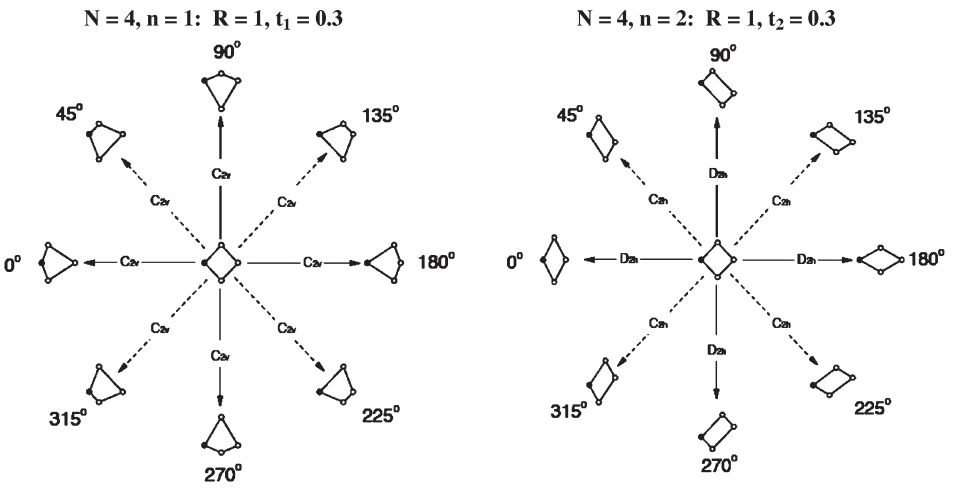

Figure 4. Pseudorotation cycles of the 4-gon.

problematic as all bonds in the ring are shifted. In this situation the following approach simplifies the analysis: Because the deformations traveling through the ring are caused by vibrational modes of specific symmetry (see Tables 1 and 2), it is easier to focus on the high symmetry forms and determine the changes associated with a symmetry element such as a C_2 axis passing through atom 1 for $\tau_n = 0$. Such an analysis reveals that it is better to speak of in-plane pseudorotation as the process where the maximum in-plane deviation from the *N*-gon is cycling through the ring without leading to any angular momentum. Nevertheless, we will use in this work the term "bond pseudorotations" as it is commonly used in the literature.

If bond pseudorotation takes place in a 2-dimensional deformation subspace and the cause for the internal process is a Jahn−Teller instability, we will speak of the associated PES as a Jahn−Teller surface. In those cases where pseudorotational subspaces are associated with degenerate vibrational modes of the same symmetry it is unlikely that a ring deformation processes is limited to one subspace. Mixing will take place so that a deformation path is defined in a larger deformation space rather than a single subspace. The contributions from the various deformation parameters can be related to special electronic effects that help to understand structural and energetic preferences.

Besides pseudorotation a deformed ring may cross directly the center of the cycle where the D_{Nh}-symmetrical form is located. Considering that in chemistry any intramolecular rearrangement that leads from the original configuration to the corresponding mirror image is called inversion (inversion of the cyclohexane chair, ammonia inversion, inversion of the configuration at an asymmetrical C atom, etc.), one is tempted to call this processes also an inversion. However, closer inspection of the deformation cycles reveals that the inversion processes proceed between equivalent forms related by a switching of bonds (see, e.g., Figure 3). Therefore, one should correctly describe deformation processes through the D_{Nh}-symmetrical form as inversions accompanied by bond-switching or "bond-switching inversions", which for reasons of simplicity we will call in the following just "inversions."

5. APPLICATION OF THE RING DEFORMATION COORDINATES

For the purpose of demonstrating the usefulness of the RDCs introduced in this work, we will discuss Jahn−Teller and other deformations in 3- and 4-rings. Calculations were carried out with the ab initio program packages COLOGNE2010,[25] CFOUR,[27] and MOLPRO.[28] We used restricted and unrestricted coupled cluster theory with all single (S) and double (D) excitations and a perturbative treatment of tritple (T) excitations, i.e., CCSD(T) and UHF-CCSD(T)[29] where the latter acronym is used to prevent confusion with unitary CC theory.[30,31] Multireference problems were treated by using MR-AQCC (multireference averaged quadratic couple cluster)[32] and EOMIP-CCSD (equation-of-motion ionization potential coupled cluster theory in the single and double excitations approximation).[33−35] All calculations were carried out with the cc-pVTZ basis set.[36] Geometry optimizations and frequency calculations were based on the use of RDCs.[37]

5.1. Cycpropane Radical Cation (1). Removal of an electron from the degenerate HOMO of cyclopropane (symmetric and antisymmetric Walsh MOs) leads to the Jahn−Teller unstable electron configuration $^2E'$, which can be stabilized by a e′-symmetrical distortion to the C_{2v}-symmetrical states $^2A_1$ and $^2B_2$ in the course of a first-order Jahn−Teller effect where the state symmetry results from the fact that either the a_1-symmetrical or the b_2-symmetrical Walsh MO is singly occupied.[9,10] Early work on the problem[38−44] was summarized, with specific consideration of bond pseudorotation, in the literature.[10] More recent work concerns the description of the ionization process, the resulting PE spectrum, and the dynamics of the Jahn−Teller distortion[45] as well as the vibronic spectra and the nonradiative decay dynamics of **1**.[46]

The cyclopropane radical cation is a multireference system, which can no longer be correctly described by single determinant theory such as DFT, HF or MP*n* with small *n*. UHF-CCSD(T) is included because infinite order excitation effects some nondynamic electron correlation,[47,48] and therefore it is able to provide a reasonable description, which, however, has to be verified by true multireference (MR) methods. We used EOMIP-CCSD[33−35] because configuration mixing in the radical cation is dominated by determinants that are related to the closed shell configuration of cyclopropane by a removal of one electron. In addition, we employed MR-AQCC with a two-state averaging based on a CASSCF reference function with a 5-electron, 6-orbital active space (MR-AQCC(5,6)) (Table 3).

At all levels of theory, the $^2A_1$ state of **1** is found as the global minimum of the Jahn−Teller PES. UHF-CCSD(T), MR-

Table 3. Calculated Ring Deformation Coordinates of 3- and 4-Membered Rings[a,b]

$C_3H_6^{+\bullet}$ [a]	sym	state	ΔE	R	t_1	τ_1	C1C2	C2C3	C3C1	C1H	C2H	HC1H	HC2H
EOMIP- CCSD	C_{2v}	$^2A_1$	0.00	0.9140	0.1395	0	1.477	1.825		1.084	1.081	117.6	118.4
	C_{2v}	$^2B_2$	2.10	0.9104	0.0963	180	1.667	1.410		1.079	1.082	120.3	118.3
	D_{3h}	$^2E'$	20.26	0.8984	0		1.556	1.556		1.082	1.082	120.6	120.6
MR- AQCC(5,6)	C_{2v}	$^2A_1$	0.00	0.9181	0.1486	0	1.478	1.848		1.083	1.081	117.0	118.5
	C_{2v}	$^2B_2$	2.39	0.9134	0.0996	180	1.675	1.410		1.079	1.082	120.8	118.2
	D_{3h}	$^2E'$	21.44	0.9002	0		1.559	1.559		1.081	1.081	120.6	120.6
UHF- CCSD(T)	C_{2v}	$^2A_1$	0.00	0.9204	0.1491	0	1.482	1.852		1.086	1.083	117.4	118.6
	C_s	$^2A'$	0.35	0.9198	0.1412	10	1.448	1.835	1.527	1.086	1.084	117.7	118.0
	C_s	$^2A'$	1.04	0.9183	0.1262	20	1.430	1.798	1.567	1.085	1.084	118.2	117.9
	C_s	$^2A'$	1.67	0.9171	0.1138	30	1.421	1.762	1.601	1.085	1.084	118.5	117.9
	C_s	$^2A'$	2.10	0.9163	0.1055	40	1.417	1.731	1.629	1.085	1.084	118.6	118.1
	C_s	$^2A'$	2.35	0.9158	0.1008	50	1.415	1.704	1.654	1.085	1.084	118.6	118.3
	C_{2v}	$^2B_2$	2.43	0.9157	0.0992	180	1.679	1.414		1.081	1.084	120.8	118.4
	D_{3h}	$^2E'$	20.92	0.9028	0		1.564	1.564		1.084	1.084	120.8	120.8

C_4H_4	sym	state	ΔE	R	t_2	τ_2	C1C2	C2C3	C1H	C2H	C1C2C3
MR- AQCC(4,4)	D_{2h} rhombic	$^1A_1$	17.48	1.0251	0.0698	0	1.453		1.082	1.071	82.2
	C_{2h}	$^1A'$	5.65	1.0238	0.0698	45	1.380	1.519	1.081	1.072	84.5
	D_{2h}	$^1A_{1g}$	0	1.0278	0.0698	90	1.355	1.552	1.077		90
	D_{4h} square	$^1A_{1g}$	7.77	1.0231	0		1.447		1.076		90

N_2S_2	sym	state	ΔE	R	t_2	τ_2	S1N2	N2S3	SS	NN	SNS
MR- AQCC(4,4)	D_{2h} rhombic	$^1A_1$	0	1.1685	0.0069	0	1.653		2.323	2.351	89.3
	C_{2h} rectangular	$^1A_{1g}$	0.36	1.1756	0.0069	90	1.650	1.677	2.352	2.352	90
	D_{2h} square	$^1A_{1g}$	0.08	1.1680	0		1.672		2.351		90
CCSD(T)	D_{2h} rhombic	$^1A_1$	0	1.1765	0.0097	0	1.664		2.372	2.333	90.9
	C_{2h}	$^1A'$	0.15	1.1765	0.0097	45	1.654	1.673	2.339	2.367	89.3
	C_{2h} rectangular	$^1A_{1g}$	0.43	1.1762	0.0097	90	1.650	1.677	2.352		90
	D_{2h} square	$^1A_{1g}$	0.17	1.1758	0		1.663		2.352		90

$N_2S_2^{2-}$	sym	state	ΔE	R	t_2	τ_2	S1N2	N2S3	SS	NN	SNS
CCSD(T)	D_{2h} rhombic	$^1A_1$	0	1.2867	0.0214	0	1.820		2.616	2.531	91.9
	C_{2h} rectangular	$^1A_{1g}$	1.07	1.2877	0.0214	90	1.791	1.851	2.576		90
	D_{2h} square	$^1A_{1g}$	0.38	1.2856	0		1.818		2.571		90

[a] Relative energies in kcal/mol, breathing radius R, amplitudes t_n, and bond lengths in Å, phase angle τ_n and bond angles in degree. [b] The irrep. is B_1 if the C3 frame is lying in the xz plane or B_2 if the C3 frame is lying in the yz plane.

AQCC(5,6), and EOMIP-CCSD place the $^2B_2$ state of radical cation **1** 2.43, 2.39, and 2.10 kcal/mol, respectively, above the $^2A_1$ state (Table 3) so that it is safe to say that the barrier for bond pseudorotation is 2.4 kcal/mol or somewhat smaller. The calculated UHF-CCSD(T) Jahn−Teller PES is shown in Figure 5. It has the 3-fold symmetry required by the D_{3h}-symmetrical parent form of **1**. Bond pseudorotation follows the dotted path with minima at $\tau = 0$, 120, and 240° and transition states at $\tau = 60$, 180, and 300°.

The calculated deformation energy surface $V(t_1,\tau_1)$ of the cyclopropane radical cation is of the general form

$$V_O(t_1,\tau_1) = V_{00} + V_{20}t_1^2 + V_{40}t_1^4 + (V_{23}t_1^2 + V_{43}t_1^4)\cos 3\tau_1 \quad (18)$$

The calculated coefficients V_{nm} are listed in Table 4. They are valid in a region $0.07 < t_1 < 0.2$ Å. For smaller values of t_1 ($t_1 < 0.07$), the Jahn−Teller bond pseudorotation potential increases steeply to a value close to 21 kcal/mol (Table 3), which is best described using an exponential function in connection with a switching function:

$$V_I(t_1,\tau_1) = A + B\exp\{Ct_1 + Dt_1\cos 3\tau_1\} \quad (19)$$

so that the total potential function results as

$$V(t_1,\tau_1) = V_I(t_1,\tau_1)\,S_I(t_1) + V_O(t_1,\tau_1)\,S_O(t_1) \quad (20)$$

$$S_I(t_1) = 1 \quad for\ t_1 \le 0.7$$
$$= 0 \quad for\ t_1 > 0.7$$

$$S_O(t_1) = 1 \quad for\ t_1 > 0.7$$
$$= 0 \quad for\ t_1 \le 0.7$$

In view of the high barrier for inversion through the 3-gon form **1** (EOMIP-CCSD: 20.26; MR-AQCC(5,6): 21.44; UHF-CCSD(T): 20.92 kcal/mol, Table 3) yielding either the 120°- or

dx.doi.org/10.1021/jp2041907 |J. Phys. Chem. A 2011, 115, 8731–8742

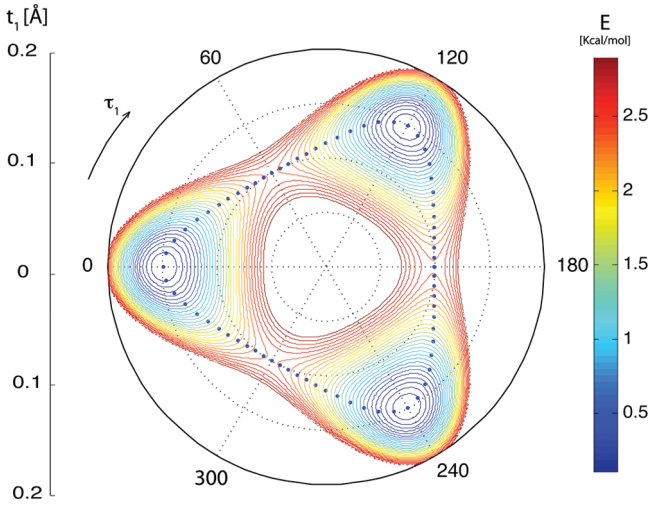

Figure 5. Bond pseudorotation (Jahn−Teller) PES of the cyclpropy radical cation spanned by RDCs $\{t_1, \tau_1\}$ (the deformation amplitude t_1 is 0 at the center, which defines the position of the D_{3h}-symmetrical form **1a**; it increases radially as indicated on the left for the 90°−270° direction). An energy scale is given on the right. All calculations at the UHF-CCSD(T)/cc-pVTZ level of theory.

240°-form (Figures 3 and 5), this process is slow at room temperature and can be excluded at lower temperatures whereas bond pseudorotation is rapid at room temperature. The e′-symmetrical Jahn−Teller deformation leads to an increase of "breathing" amplitude $t_0 = R - R_0$ from 0 to 0.0156, 0.0179, and 0.0176 Å for EOMIP-CCSD, MR-AQCC(5,6), and UHF-CCSD(T) (Table 3), which reflects the fact that the CC bonds become longer by the value of t_0 on the average. At the same time the deformation amplitude t_1 increases from 0 to 0.14 and 0.15 Å for the $^2A_1$-forms, which indicates the deformation of the cyclopropane framework to a biradicaloid state close to the trimethylene biradical, which, contrary to the latter, possesses still some stabilizing interactions between the separated C atoms. In the literature, some experimental results were discussed in favor of the generation of the trimethylene biradical;[41] however, this could not be confirmed by quantum chemical calculations and it is more likely that **1**($^2A_1$) had been observed, which is known to be the starting point for the formation of the propenyl radical cation.[42,43] The $^2B_2$ transition state for bond pseudorotation has been considered because of its similarity with a methylene-ethene π-complex to be a starting point for the dissociation into methylene and the ethene radical cation,[43] which would imply two transition states in sequence.

We note that different electronic factors caused by substituents can stabilize either the minima or the transition states of bond pseudorotation. π-Donor−σ-acceptor substituents at C2 and C3 will lower the barrier so that **1** approaches a free pseudorotor whereas π-acceptor substituents at C1 lead to a stabilization of the minima forms thus increasing the barrier.

In view of the rapid bond pseudorotation with a barrier of just 2.4 kcal/mol, all measured properties, e.g., hyperfine structure constants, are time-averaged properties, which make it difficult to draw any conclusion with regard to the electronic structure of **1**. This problem can be solved with the help of the calculated Jahn−Teller surface shown in Figure 5. By calculating the property in question as a function of the pseudorotation phase angle τ_1, then assuming a Boltzmann statistic, and utilizing the

Table 4. Calculatd Ring Deformation Surfaces[a]

$C_3H_5^{+\bullet}$, **1**		C_4H_4, **2**		N_2S_2, **3**		$N_2S_2^{2-}$, **4**	
V_{00}	4.352	V_{00}	7.497	V_{00}	0.169	V_{00}	0.377
V_{20}	−392.494	V_{20}	−450.877	V_{20}	1789.550	V_{20}	816.272
V_{40}	14404.531	V_{40}	137658.306	V_{40}	−11495.326	V_{40}	−14373.243
V_{23}	0.721	V_{22}	3134.050	V_{11}	−34.884	V_{11}	−35.258
V_{43}	−5593.033	V_{42}	−365686.575	V_{22}	1027.009	V_{22}	711.196
		V_{62}	18533094.659	V_{31}	443.555	V_{31}	644.052
A	−0.863						
B	21.794						
C	−0.158						
D	−22.138						

[a] Coefficients V_{nm} in (kcal/mol) Å^{-n}; A and B in kcal/mol; C and D in (kcal/mol) Å^{-n}. For **1**, the potential is given in eqs 18 and 19. For all other compounds, the first subscript of V indicates the power of the deformation amplitude t and the second the prefactor m of the deformation phase angle in cos $m\tau$.

calculated potential of the Jahn−Teller-PES, we can determine time-averaged properties, which can be directly compared with measured data. In this way, it is possible to analyze the corresponding measured data. This is the basis of the DORCO method, which one of us has successfully used to determine from time-averaged NMR spin−spin coupling constants the puckering of a pseudoroting ring.[49] Also the investigation of dynamic processes involving both ground and excited states of **1**[45,46] will be simplified by taking advantage of calculated Jahn−Teller surfaces for the different states.

5.2. Cyclobutadiene (2). The description of bond pseudorotation in the cyclopropane radical cation can be generalized to any other planar ring. Most interesting in this connection are planar monocyclic polyenes with a positive charge and a degenerate Jahn−Teller unstable ground state.[37] Another example is the D_{4h}-symmetrical cyclobutadiene molecule **2a** that becuase of a pseudo-Jahn−Teller effect undergoes distortion to the rectangular form **2a**.[9] There are numerous quantum chemical investigations that have determined the energy difference between **2a** and **2b** and calculated their geometries and other properties.[50−63] However, none of these investigations has considered the deformation surface of **2** and the possibility that the 4-ring can also undergo bond pseudorotation.

For the 4-ring, there exist two different deformation cycles shown in Figure 4: the first one is the kite-isoceles trapezoid cycle ($n = 1$) and the second one the rhombus-parallelogram-rectangle cycle ($n = 2$). Hence, the deformation surface is 5-dimensional (2 pseudorotational subspaces and the 1-dimensional breathing subspace with $n = 0$). Because of the high symmetry of **2**, deformations preferentially take place in parts of the subspaces with $n = 0$ and $n = 2$. The observed bond shifting process of **2b** proceeds in the form of an inversion via the square form **2a** (Figure 4, $n = 2$). According to the MR-AQCC(4,4)/cc-pVTZ calculations carried out in this work, the barrier for this process is 7.8 kcal/mol, in good agreement with recent calculations.[50−55] Breathing (t_0 expansion by 0.005 Å) and deformation for a fixed $\tau_2 = 90$ or 270° and $t_2 = 0.070$ Å take place at the same time where the former process contributes just 7% to the total deformation. Imposing the same t_2-deformation on the cyclobutadiene rhombus leads to a 0.003 Å contraction of the ring and an increase in energy by 17.5 kcal/mol relative to **2b**. This reflects the fact that a

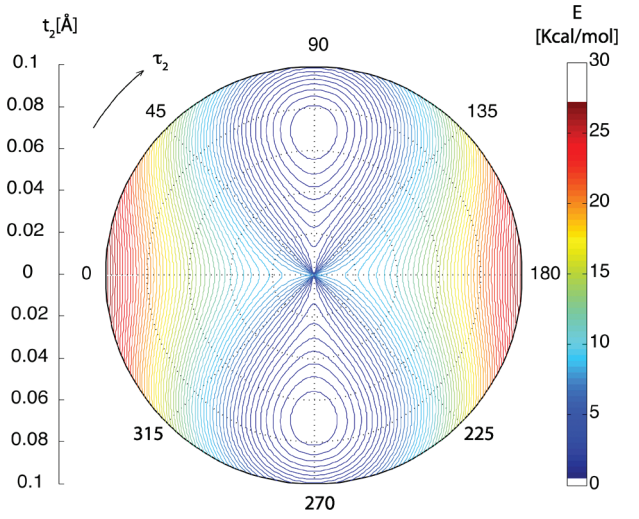

Figure 6. Bond pseudorotation (Jahn−Teller) PES of cyclobutadiene calculated at the MR-AQCC(4,4)/cc-pVTZ level of theory. Minima are located at τ_2 = 90 and 270°. See Figure 2 for further explanations. Compare also with Figure 1, n = 2.

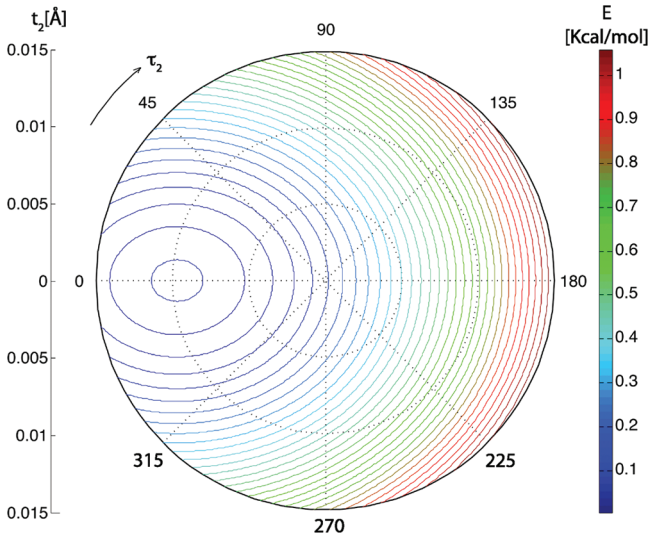

Figure 7. Bond pseudorotation PES of N_2S_2 calculated at the CCSD-(T)/cc-pVTZ level of theory. The minimum is located at τ_2 = 0°, t_1 = 0.0097 Å of a flat surface. See Figure 2 for further explanations.

b_{1g}-symmetrical deformation changes the nonbonded rather than the bonded distances in cyclobutadiene, which does not lead to an effective separation of pseudodegenerate states $^1B_{1g}$ and $^1B_{2g}$ and subsequent stabilization. The potential function increases for increasing t_2 in the 0°-to-180° direction of τ_2 where this increase is quadratic, reaching a value of 21 kcal/mol at t_2 = 0.08 Å. This is in line with the fact that the square form **2a** is a first-order transition state for the bond shift reaction. The t_2-deformation of **2b** applied for τ_2 = 45° (parallelogram, Figure 4) leads to an increase in energy of just 5.6 kcal/mol, thus revealing that the parallelogram form is stabilized relative to **2a**. This reflects the fact that b_{1g}- and b_{2g}-symmetrical deformations are equally mixed for τ_2 = 45° and that b_{2g}-symmetrical deformation increases the energy difference between the pseudodegenerate states.

The calculated Jahn−Teller surface of **2** is shown in Figure 6, and the corresponding potential, in Table 4. The MR-AQQCC-(4,4) calculations reveal that at normal temperatures larger parts of the Jahn−Teller surface are energetically accessible and that bond shifting can also involve some bond pseudorotation at slightly higher energies than that of **2a**. Push−pull substituents can change the surface and make rhombic forms accessible. In recent work, Eckert-Maksic and co-workers[51] have documented the lowering of the barrier for inversion via **2a** in the case of cyano-substituted **2** and McMahon and co-workers[50] have shown that 1- and 1,3-cycano-substitution leads to the rhombic forms of **2**.

5.3. Disulfur Dinitride and Its Dianion (3 and 4). A priori one should not expect disulfur dinitride **3** to adopt a square form because S and N prefer different bond orbital arrangements. However, X-ray studies have described the geometry of N2S2 as being close to that of a square (NS bond lengths of 1.651 and 1.657 Å; NSN and SNS angles of 90.4 and 89.6°, respectively[64−66]). This seems to be in line with the assumption that **3** represents a Hückel-aromatic 6π-electron system.[67] Calculations based on spin-coupled valence-bond theory and the CISD methods,[68,69] however, suggest biradical character for **3** with a weak singlet-coupling across the 4-ring between the S atoms in line with early suggestions based on more qualitative considerations.[70] This description has been challenged by Schleyer and co-workers, who have pointed out that a direct confirmation of biradical character in terms of natural orbital occupation numbers has never been given.[71] These authors find on the basis of the valence space optimized doubles method that **3** is a 2π-aromatic molecule with a low aromatic stabilization energy of just 6.5 kcal/mol, NS bond orders of 1.25, and some weak biradical character of just 12%.[71] Two of the six π-electrons are in the bonding MO whereas the remaining π-electrons occupy nonbonding MOs (see Figure 8).

The CCSD(T) equilibrium geometry of **3** calculated in this work confirms a D_{2h}-symmetrical rhombic form (τ_2 = 0°) close to the experimental geometry and the ideal square form **3a**. The small deviation from **3a** is reflected by the calculated deformation parameters t_0 = 0.0007 and t_2 = 0.0097 Å. By imposing an incomplete bond pseudorotation to the rectangular form at frozen t_2, we obtain only a small increase in energy of 0.43 kcal/mol. The calculated pseudorotation surface shown in Figure 7 is very flat. At room temperature, a heat content of 0.6 kcal/mol will make large parts of the deformation surface accessible for **3**, which can carry out ring inversions, bond pseudorotation, librations, and other movements. Our calculations show, however, that these movements will not lead to a major change in the electronic structure of **3**, for example by substantially increasing its biradical character.

If two electrons are added, thus leading to the disulfur dinitride dianion **4**, an 8π-electron system is obtained that might be considered as being antiaromatic. However, antiaromaticity is invoked by partial occupancy of a set of degenerate π-MOs, which is not the case for **4** (Figure 8). Instead, an NS-antibonding $2b_{1u}$-symmetrical π-MO is doubly occupied (see Figure 8), thus leading to a weakening of the NS bonds that lengthen from 1.664 Å in **3** to 1.820 Å in **4** (Table 3). Apart from this bond weakening, **4** has deformation properties similar to those of the neutral molecule **3**, as is reflected by the calculated deformation parameters and the deformation surface (Tables 3 and 4) that hardly differs from that of **3** (Figure 7). The energy differences between

dx.doi.org/10.1021/jp2041907 |J. Phys. Chem. A 2011, 115, 8731–8742

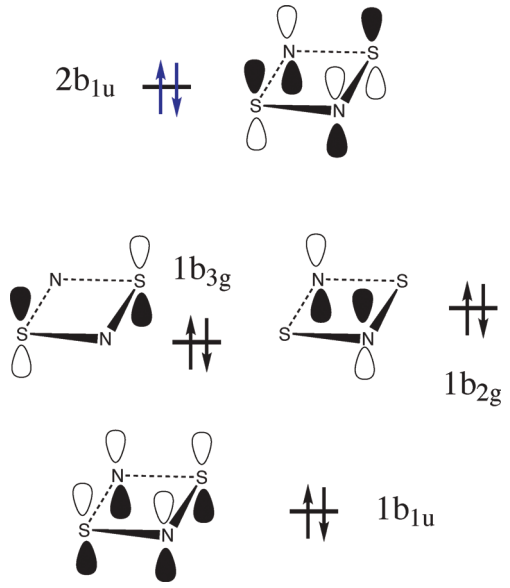

Figure 8. π-Molecular orbitals occupied by 6 electrons in N_2S_2 (black arrows) and its dianion. The additional two electrons in the dianion are given in blue.

the deformation forms listed in Table 3 differ by a factor of 2, which still makes dianion **4** a floppy molecule with large deformation motions.

5.4. Normal Coordinates and Deformation Coordinates. Because the RDCs are derived from the normal vibrational modes of a planar ring, the question may arise whether the use of normal rather than deformation coordinates could lead to a similar description of deformed rings. Indeed, such an approach was performed by Liehr[8,72] and is also described by Bersuker.[9] There are a number of reasons why RDCs are superior to normal coordinates when deformed ring molecules are described. Normal coordinates depend on the number N of ring atoms, symmetry, atomic masses, interactions between ring and substituent atoms, and the deviation of the ring molecule from planarity. There is no simple way of deriving normal coordinates for C_1-symmetrical ring systems with varying N so that they can easily be used to carry out energy, geometry, or vibrational frequency calculations for a given deformation. The RDCs developed do not suffer from these problems: (i) They are defined for any ring irrespective of its size by two simple formulas. Each RDC has a clear mathematical and geometrical meaning. (ii) They do not depend on symmetry, mass, or the interactions of ring atoms and substituent atoms. (iii) Analytical first and second energy derivatives in terms of RDCs are easily determined and have already been used in the geometry optimizations and vibrational frequency calculations presented in this work. (iv) If a given deformation of the ring has to be investigated, this can be easily specified utilizing the RDCs; all remaining independent coordinates are then optimized. Any number of energy points needed for determining the energy dependence of bond pseudorotation or other deformation processes can be specified for a ring molecule (irrespective of N, symmetry, substituents, etc.). (v) Deformations of different rings become comparable via their RDCs, which in turn can be associated with electronic effects. (vi) RDCs quantify the electronic effects of substituents on a ring molecule and facilitate the electronic analysis of deformed rings.

The RDC complement the ring puckering coordinates of Cremer and Pople,[17] which have been extensively used in the literature as they are superior to normal coordinates when the pucker of a ring molecule is described. Any ring molecule can be exclusively described by puckering and deformation coordinates, which is always then of advantage when a conformational process of a ring molecule or a ring form of specified pucker and deformation has to be described.

6. CONCLUSIONS

In this work, we have developed a new way of describing in-plane deformations of planar rings with a set of ring deformation coordinates (RDC):

(1) The RDCs are directly derived from the in-plane normal vibrational modes of the ring. For an N-ring, there are $2N - 3$ RDCs that are sufficient to describe the geometry of a planar ring without using bond lengths or bond angles. By using the RDCs rather than bond lengths and bond angles, we solve the redundancy problem of ring molecules with N bond lengths and N internal ring angles.

(2) The RDCs are defined with regard to the N-gon of unit length as reference ring in a way similar to that of the planar ring itself is the reference for the puckered ring. The $(2N - 3)$ RDCs partition the deformation space of a ring molecule into a 1-dimensional "ring-breathing" subspace, spanned by the breathing parameter R, and $(N - 2)$ 2-dimensional pseudorotational subspaces, each spanned by a deformation amplitude t and a phase angle τ.

(3) The pseudorotational subspaces $n = 1, ..., (N - 2)$ define, irrespective of N, ring deformations that are found to change systematically with n: They deform the N-ring so that the impression of an $M = N - n$ ring is given. For the largest value of $n = (N - 2)$, the deformation with $M = 2$ is obtained, resembling an elliptically deformed circle (2-gon). We note that the deformation vectors and the corresponding RDCs are directly derived from the in-plane vibrational modes, which lead to the same pattern.

(4) The two RDCs that span a 2-dimensional deformation space can also be used to define, for each n, two basis forms with high symmetry. All other deformed rings in the 2-dimensional subspace can be viewed as linear combinations of the basis forms.

(5) Utilizing the RDCs and the pseudorotational subspaces they span, dynamic deformation processes can be described in a unique way. The investigation of 3- and 4-rings reveals that the double bond shift in rectangular cyclobutadiene corresponds to a ring inversion of the planar ring involving the square form whereas this process in an odd-membered ring is better described as bond-stretch isomerization via a D_{Nh}-symmetrical form, which can involve more than one bond. Bond pseudorotation turns out to be a constrained bond-stretching followed by a bond-switching for high-symmetry forms.

(6) Any complete set of internal or Cartesian coordinates of a planar N-ring can be transformed into $(2N - 3)$ RDCs. In turn, RDCs can be used to derive the internal or Cartesian coordinates of the ring. Programs that carry out the transformation are provided as free software.[26]

(7) The RDCs can be utilized to determine Jahn–Teller surfaces or deformation surfaces in analytical form. This is

possible because any given deformation coordinate can be frozen and the remaining deformation coordinates optimized. In a separate work, we will present the analytical energy gradient and Hessian expressed in deformation coordinates.[37]

(8) Application of the RDCs made it possible to calculate the Jahn−Teller or deformation surfaces for the cyclopropyl radical cation, cyclobutadiene, disulfur dinitride, and dianion of the latter thus gaining the following insights: (a) Bond pseudorotation in a 3-ring is best viewed as a combination of bond stretching and bond switching of equally stretched bonds at the transition states of the rearrangement. Bond pseudorotation is only hindered by a barrier of 2 kcal/mol in the cyclopropyl radical cation. It leads to a rearrangement of the ring from biradicaloid minima with some trimethylene character to methylene−ethene cation π-complexes as was already observed by other authors.[10] Appropriate substitution will lead to free bond pseudorotation. (b) Cyclobutadiene can undergo besides the well-known bond stretch isomerization via the square form (inversion-process) also bond pseudorotation involving rhombic forms. These rearrangements require in the parent compound some additional energy (slightly above the isomerization barrier of 7.8 kcal/mol) but should become the preferred process in substituted cyclobutadienes of lower than D_{2h}-symmetry. (c) The calculated deformation surfaces of disulfur dinitride and its dianion reveal large deformational flexibility typical of floppy molecules. This, however, does not lead to a specific change of their electronic character: The molecules retain their 2π-aromatic nature without a significant contribution of biradical character.

In conclusion, we see a broad application spectrum of the RDCs developed in this work: (a) For the first time dynamic Jahn−Teller processes can be described on the basis of calculating the corresponding PES. The same set of coordinates can also be used to describe Jahn−Teller deformations in planar acyclic molecules of the type AX_n. (b) The RDCs provide also suitable descriptors for opening/closure reactions of planar rings. (c) As previously shown in the case of the puckering coordinates,[21] the deformation amplitudes can be used to express the degree of deformation in percent and then to compare deformations in ring systems of different structure and different size. Processes leading to a crossing from one deformation subspace to another can be described by introducing hyperspherical angles as done in the case of puckering processes.[21] (d) Ring substituents lead to a deformation of the ring structure due to the electronic effects they exert on the ring atoms. These deformations can be analyzed in terms of RDCs, then associated with specific deformation modes, and finally used to provide a detailed description of electronic effects induced by the substituents. (e) The concept of the RDCs can be extended to a description of processes such as Berry pseudorotation[73] or deformations in fullerenes caused by ionization, electron attachment, or substitution.

Finally it should be noted that any puckered ring molecules can be completely described by a set of $N - 3$ puckering coordinates and $2N - 3$ deformation coordinates without using a single bond length, bond angle, or dihedral angle. In this way, ring forms of exactly specified pucker and deformation can be investigated. In work under progress, we will demonstrate the advantages of such an approach.

■ ASSOCIATED CONTENT

Supporting Information. Appendix with additional information on ring deformation and ring puckering coordinates and their relationship to the irreducible representations of the D_{Nh} point group (see Table A.1). Pseudorotation cycles of some larger rings (Figures A.1−A.4) that help to visualize the dierent deformation modes and the eect of the deformations on the ring form. Derived relationship between mode n of the N-ring and its deformations. This material is available free of charge via the Internet at http://pubs.acs.org.

■ AUTHOR INFORMATION

Corresponding Author
*E-mail: dcremer.at.smu.edu.

■ ACKNOWLEDGMENT

This work was financially supported by the National Science Foundation, Grant CHE 071893. We thank SMU for providing computational resources. Some early work on the symmetry of deformed rings was carried out by Nils Calander when being guest of the CATCO group.

■ REFERENCES

(1) Cremer, D.; Kraka, E. *Curr. Org. Chem.* **2010**, *14*, 1524–1560.
(2) Kraka, E. In *Encyclopedia of Computational Chemistry, Vol 4*; Schleyer, P. v. R., Allinger, N. L., Clark, T., Gasteiger, J., Kollman, P. A., Schaefer III, H. F., Schreiner, P. R., Eds.; John Wiley, Chichester, UK, 1998; p 2437.
(3) Kraka, E. In *Wiley Interdisciplinary Reviews: Computational Molecular Science, Reaction Path Hamiltonian and the Unified Reaction Valley Approach*,; Allen, W., Schreiner, P. R., Eds.; Wiley, New York, 2011; p xx.
(4) Cremer, D.; Larsson, J. A.; Kraka, E. In *Theoretical and Computational Chemistry, Vol. 5, Theoretical Organic Chemistry*; Parkanyi, C., Ed.; Elsevier, Amsterdam, 1998; p 259.
(5) Konkoli, Z.; Cremer, D. *Int. J. Quantum Chem.* **1998**, *67*, 1–9.
(6) Konkoli, Z.; Cremer, D. *Int. J. Quantum Chem.* **1998**, *67*, 29–40.
(7) Herzberg, G. *Molecular Spectra and Molecular Structure, III. Electronic Spectra and Electronic Structure of Polyatomic Molecules*; Van Nostrand, New York, 1966.
(8) Liehr, A. D. *J. Phys. Chem.* **1963**, *67*, 389–471.
(9) Bersuker, I. B. *The Jahn-Teller Effect*; Cambridge University Press, Cambridge, 2006.
(10) Cremer, D.; Kraka, E.; Szabo, K. J. In *The Chemistry of Functional Groups, The Chemistry of the Cyclopropyl Group, Vol. 2*; Rappoport, Z., Ed.; John Wiley, New York, 1995; p 43.
(11) Minkin, V.; Glukhovtsev, M. N.; Simkin, B. Y. *Aromaticity and Antiaromaticity, Electronic and Structural Aspects*; Wiley, New York, 1994.
(12) Paquette, L. A.; Gardlik, J. M.; Johnson, L. K.; McCullough, K. J. *J. Am. Chem. Soc.* **1980**, *102*, 5026–5032.
(13) Paquette, L. A.; Wang, T.-Z.; Luo, J.; Cottrell, C. E.; Clough, A. E. *J. Am. Chem. Soc.* **1990**, *112*, 239–253.
(14) Pemberton, R. P.; McShane, C. M.; Castro, C.; Karney, W. L. *J. Am. Chem. Soc.* **2006**, *128*, 16692–16700.
(15) Castro, C.; Karney, W. L.; McShane, C. M.; Pemberton, R. P. *J. Org. Chem.* **2001**, *71*, 6795–6800.
(16) Moll, J. F.; Pemberton, R. P.; Gutierrez, M. G.; Castro, C.; Karney, W. L. *J. Am. Chem. Soc.* **2007**, *129*, 274–275.
(17) Cremer, D.; Pople, J. A. *J. Am. Chem. Soc.* **1975**, *97*, 1354–1358.
(18) Cremer, D.; Pople, J. A. *J. Am. Chem. Soc.* **1975**, *97*, 1358–1367.
(19) Cremer, D. *J. Chem. Phys.* **1979**, *70*, 1898–1910.
(20) Cremer, D. *Israel J. Chem.* **1983**, *23*, 72–84.

(21) Cremer, D.; Szabo, K. J. In *Methods in Stereochemical Analysis, Conformational Behavior of Six-Membered Rings, Analysis, Dynamics, and Stereoelectronic Effects*; Juaristi, E., Ed.; VCH Publishers, 1995; p 59.
(22) Cremer, D. *J. Phys. Chem.* **1990**, *94*, 5502–5509.
(23) Wilson, E. B.; Decius, J. C.; Cross, P. C. *Molecular Vibrations*; McGraw-Hill, New York, 1955.
(24) Pickett, H. M.; Strauss, H. L. *J. Chem. Phys.* **1971**, *55*, 324–334.
(25) Kraka, E.; Gräfenstein, J.; Filatov, M.; Zou,W.; Joo, H.; Izotov, D.; Gauss, J.; He, Y.;Wu, A.; Polo, V.; Olsson, L.; Konkoli, Z.; He, Z.; Cremer, D. COLOGNE2010. 2010; Southern Methodist University, Dallas, TX.
(26) Cremer, D.; Izotov, D.; Zou,W.; Kraka, E. RING, a coordinate transformation program. 2011; Southern Methodist University, Dallas, TX.
(27) Stanton, J. F.; Gauss, J.; Harding, M. E.; Szalay, P. G.; et al. , CFOUR, a quantum chemical program package. 2010; see http://www.cfour.de.
(28) Werner, H. J.; Knowles, P. J.; Kniza, G.; Manby, F. R.; Schütz, M.; other, MOLPRO, version 2010.1, a package of ab initio programs. 2010; see http://www.molpro.net.
(29) Raghavachari, K.; Trucks, G. W.; Pople, J. A.; Head-Gordon, M. *Chem. Phys. Lett.* **1989**, *157*, 479–483.
(30) Mukherjee, D.; Moitra, R. K.; Mukhopadhayay, A. *Mol. Phys.* **1975**, *30*, 1861–1888.
(31) Kutzelnigg, W. *J. Chem. Phys.* **1982**, *77*, 3081–3097.
(32) Szalay, P. G.; Bartlett, R. *J. Chem. Phys. Lett.* **1993**, *214*, 481–488.
(33) Nooijen, M.; Snijders, J. G. *Int. J. Quantum Chem., Quantum Chem. Symp.* **1992**, *26*, 55–83.
(34) Nooijen, M.; Snijders, J. G. *Int. J. Quantum Chem.* **1993**, *48*, 15–48.
(35) Stanton, J. F.; Gauss, J. *J. Chem. Phys.* **1994**, *101*, 8938–8944.
(36) Dunning, T. H. *J. Chem. Phys.* **1989**, *90*, 1007–1023.
(37) Zou, W.; Izotov, D.; Cremer, D. *J. Chem. Phys.* **2011**, xx–xx.
(38) Roth, H. D.; Schilling, M. L. M. *Can. J. Chem.* **1983**, *61*, 1027–1035.
(39) Qin, X.-Z.; Williams, F. *Chem. Phys. Lett.* **1984**, *112*, 79–83.
(40) Roth, H. D.; Schilling, M. L. M.; Schilling, F. C. *J. Am. Chem. Soc.* **1985**, *107*, 4152–4158.
(41) Sack, T. M.; Miller, D. L.; Gross, M. L. *J. Am. Chem. Soc.* **1985**, *107*, 6795–6800.
(42) Du, P.; Hrovat, D. A.; Borden, W. T. *J. Am. Chem. Soc.* **1988**, *110*, 3405–3412.
(43) Skancke, A. *J. Phys. Chem.* **1995**, *99*, 13886–13889.
(44) Hofmann, M.; Schaefer, H. F., III *J. Mol. Struct.* **2001**, *599*, 95–116.
(45) Venkatesan, T. S.; Mahapatra, S.; Cederbaum, L. S.; Köppel, H. *J. Phys. Chem. A* **2004**, *108*, 2256–2267.
(46) Venkatesan, T. S.; Mahapatra, S.; Meyer, H.-D.; Köppel, H.; Cederbaum, L. S. *J. Phys. Chem. A* **2007**, *111*, 1746–1761.
(47) He, Z.; Cremer, D. *Int. J. Quant. Chem. Quant. Chem. Symp.* **1991**, *25*, 43–70.
(48) He, Z.; Cremer, D. *Theoret. Chim. Acta* **1993**, *85*, 305–323.
(49) Wu, A.; Cremer, D. *J. Phys. Chem. A* **2003**, *107*, 1797–1810.
(50) Menke, J. L.; Patterson, E. V.; McMahon, R. J. *J. Phys. Chem. A* **2010**, *114*, 6431–6437.
(51) Eckert-Maksic, M.; Lischka, H.; Maksic, Z. B.; Vazdar, M. *J. Phys. Chem. A* **2009**, *113*, 8351–8358.
(52) Karadakov, P. B. *J. Phys. Chem. A* **2008**, *112*, 7303–7309.
(53) Cremer, D.; Kraka, E.; Joo, H.; Stearns, J. A.; Zwier, T. S. *Phys. Chem. Chem. Phys.* **2006**, *8*, 5304–5316.
(54) Eckert-Maksic, M.; Vazdar, M.; Barbatti, M.; Lischka, H.; Maksic, Z. B. *J. Chem. Phys.* **2006**, *125*, 064310−1–064310−9.
(55) Demel, O.; Pittner, J. *J. Chem. Phys.* **2006**, *124*, 144112–1 − 144112−7.
(56) Levchenko, S. V.; Krylov, A. I. *J. Chem. Phys.* **2004**, *120*, 175–185.
(57) Mo, Y. R.; Schleyer, P. v. R. *Chem.—Eur. J.* **2006**, *12*, 2009–2020.
(58) Maksic, Z. B.; Kovacevi, B.; Lesar, A. *Chem. Phys.* **2000**, *253*, 59–71.
(59) Sanchion-Garcia, J. C.; Perez-Jimenez, A. J.; Moscardo, F. *Chem. Phys. Lett.* **2000**, *317*, 245–251.
(60) Balci, M.; McKee, M. L.; Schleyer, P. v. R. *J. Phys. Chem. A* **2000**, *104*, 1246–1255.
(61) Glukhovtsev, M. N.; Laiter, S.; Pross, A. *J. Phys. Chem.* **1995**, *99*, 6828–6831.
(62) Arnold, B. R.; Michl, J. *J. Phys. Chem.* **1993**, *97*, 13348–13354.
(63) Wright, S. C.; Cooper, D. L.; Geratt, J.; Raimundi, M. *J. Phys. Chem.* **1992**, *96*, 7943–7952.
(64) Greenwood, N. N.; *Earnshaw, Chemistry of the Elements*; Pergamon Press, Oxford, 1984.
(65) Mikulski, C. M.; Russo, P. J.; Saran, A. G.; MacDiarmid, M. S.; Garito, A. F.; Heeger, A. F. *J. Am. Chem. Soc.* **1975**, *97*, 6358–6363.
(66) MacDiarmid, A. G.; Mikulski, C. M.; Russo, P. J.; Saran, M. S.; Garito, A. F.; Heeger, A. J. *J. Chem. Soc. Chem. Commun.* **1975**, 476–477.
(67) Herler, S.; Mayer, P.; Noth, H.; Schulz, A.; Suter, X.; Vogt, M. *Angew. Chem., Int. Ed.* **2001**, *40*, 3173–3175.
(68) Gerratt, J.; McNicholas, S. J.; Sironi, M.; Cooper, D. L.; Karadakov, P. B. *J. Am. Chem. Soc.* **1996**, *118*, 6472–6476.
(69) Harcourt, R. D.; Klapotke, T. M.; Schulz, A.; Wolynec, P. *J. Phys. Chem. A* **1998**, *102*, 1850–1853.
(70) Skrezenek, F. L.; Harcourt, R. D. *J. Am. Chem. Soc.* **1984**, *106*, 3934–3936.
(71) Jung, Y.; Heine, T.; Schleyer, P. v. R.; Head-Gordon, M. *J. Am. Chem. Soc.* **2004**, *126*, 3132–3138.
(72) Liehr, A. D. *J. Phys. Chem.* **1963**, *67*, 472–494.
(73) Berry, R. S. *J. Chem. Phys.* **1960**, *32*, 933–938.